THE JOURNAL OF PHYSICAL CHEMISTRY B

Article

pubs.acs.org/JPCB

2-Propanol As a Co-Guest of Structure II Hydrates in the Presence of Help Gases

Youngjun Lee,[†] Seungmin Lee,[‡] Sungwon Park,[†] Yunju Kim,[†] Jong-Won Lee,[§] and Yongwon Seo*[,†]

[†]School of Urban and Environmental Engineering, Ulsan National Institute of Science and Technology, Ulsan 689-798, Republic of Korea

[‡]Green Technology Center, Korea Institute of Industrial Technology, Ulsan 681-310, Republic of Korea

[§]Department of Environmental Engineering, Kongju National University, Chungnam 331-717, Republic of Korea

Supporting Information

ABSTRACT: The enclathration of 2-propanol (2-PrOH) as a co-guest of structure II (sII) hydrates in the presence of CH_4 and CO_2 was experimentally verified with a focus on macroscopic phase behaviors and microscopic analytical methods such as powder X-ray diffraction (PXRD) and NMR spectroscopy. 2-PrOH functioned as a hydrate promoter in the CH_4 + 2-PrOH systems, whereas it functioned as an apparent hydrate inhibitor in the CO_2 + 2-PrOH systems despite the inclusion of 2-PrOH in the hydrate lattices. From the PXRD patterns, both double CH_4 + 2-PrOH and double CO_2 + 2-PrOH hydrates were identified to be cubic ($Fd3m$) sII hydrates. From the ^{13}C NMR spectra, it was found that, at a lower 2-PrOH concentration, the small 5^{12} cages of the sII hydrate were occupied by CH_4 molecules only, whereas the large $5^{12}6^4$ cages were shared by CH_4 and 2-PrOH molecules. However, at a stoichiometric concentration, the large cages were occupied by 2-PrOH molecules only, and the corresponding chemical formula for this concentration is $1.50CH_4 \cdot 0.98$ 2-PrOH$\cdot 17H_2O$.

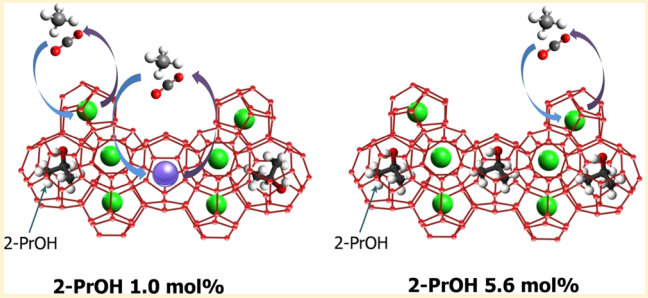

INTRODUCTION

Gas hydrates are nonstoichiometric crystalline compounds formed when guest molecules of suitable size and shape are incorporated into the well-defined cages in the host lattice constructed from hydrogen-bonded water molecules.[1] Gas hydrates exist in three different crystal structures of sI, sII, and sH, which contain differently sized and shaped cages that primarily depend on the molecular sizes of the guest species.[1] Generally, guest molecules such as CH_4 or CO_2 form sI hydrates, and much larger guest molecules such as C_3H_8 or THF form sII hydrates. In addition, large liquid hydrocarbon molecules such as neohexane or methylcyclohexane form sH hydrates in the presence of help gases.[1] Gas hydrates are of particular concern in the petroleum industry, as well as in the energy and environmental fields. In particular, gas hydrates pose a significant problem in the oil and gas industries as they can block valves, well heads, and pipelines, which can cause loss of production, damage to equipment, and possible leakage of oil and gas. Extensive efforts have been made in developing hydrate inhibitors that avoid hydrate plugging using various methods.[1,2] The most convenient method that has been adopted by the petroleum and gas industries is the introduction of well-known thermodynamic hydrate inhibitors, such as methanol and glycols, into the pipelines. The addition of a sufficient amount of thermodynamic hydrate inhibitors shifts the conditions required for hydrate formation into unfavorable regions represented by lower temperatures and higher pressures; thus, this can prevent the formation of gas hydrates. Methanol, a hydrophilic molecule, generally disrupts the hydrogen bonding network of water and inhibits gas hydrate formation without being captured in the cages of gas hydrates. However, it has been recently observed that alcohols such as ethanol, 1-propanol, 2-propanol, and *tert*-butanol form sII hydrates in the presence of a hydrophobic gas such as methane.[3−15] This indicates that alcohol molecules can also be guests of hydrate lattices in the presence of help gases; furthermore, it can function as a thermodynamic hydrate promoter for the gas hydrate formation.

Several researchers have demonstrated that 2-propanol (2-PrOH), a secondary alcohol, forms two types of simple clathrate hydrates with water at temperatures well below the freezing point of water; the corresponding stoichiometries of each 2-PrOH hydrate are 2-PrOH$\cdot 5H_2O$ and 2-PrOH$\cdot 4.75H_2O$, respectively, and with the pressurization of CH_4, forms double CH_4 + 2-PrOH hydrates at elevated pressures.[11−16] Modeling and molecular dynamics studies, Raman spectroscopic measurements, and powder X-ray diffraction (PXRD) studies have suggested that the 2-PrOH molecules form sII hydrates in the presence of CH_4 and can be captured in the large $5^{12}6^4$ cages.[11−14] However, the guest distribution behavior

Received: October 23, 2012
Revised: January 21, 2013
Published: February 12, 2013

dx.doi.org/10.1021/jp310487w | *J. Phys. Chem. B* 2013, 117, 2449−2455

and cage occupancies of guest molecules in the double CH_4 + 2-PrOH hydrates with various 2-PrOH concentrations remain unclear. In addition, CO_2 has not yet been adopted as a help gas for the formation of the double 2-PrOH hydrates.

In this study, the precise nature and unique pattern of the double 2-PrOH hydrates formed in the presence of CH_4 and CO_2 as help gases were investigated through macroscopic stability condition measurements and microscopic NMR and PXRD analyses. The three-phase hydrate equilibria (clathrate hydrate (H)−liquid water (L_W)−vapor (V)) for the ternary CH_4 + 2-PrOH + water and CO_2 + 2-PrOH + water mixtures at four different 2-PrOH concentrations (1.0, 5.6, 10.0, and 15.0 mol %) were measured in order to determine the hydrate stability conditions. The structure identification of both the double CH_4 + 2-PrOH and double CO_2 + 2-PrOH hydrates was undertaken via PXRD in order to confirm the structural transition due to the enclathration of the 2-PrOH molecules. The guest distributions and cage occupancies in the double CH_4 + 2-PrOH hydrates were examined via ^{13}C NMR spectroscopy at a concentration lower than stoichiometry, as well as at the stoichiometric concentration, of sII hydrate.

EXPERIMENTAL METHODS

Materials. The CH_4 and CO_2 gases used for the present study were supplied by Union Gas (Republic of Korea) and had a stated purity of 99.95 and 99.99%, respectively. 2-PrOH with a purity of 99.5% was purchased from Sigma-Aldrich (USA). Double-distilled deionized water was used. All materials were used without further purification.

Apparatus and Procedures. The experimental apparatus for the hydrate phase equilibria was specially designed to accurately measure the hydrate dissociation pressures and temperatures. The equilibrium cell was made of 316 stainless steel and had an internal volume of about 200 cm^3 and immersed in the water bath. The water bath temperature was controlled by a refrigerating and heating circulator with temperature programmable controller (RW-2025G, JEIO Tech, Republic of Korea). Two sapphire windows equipped in the front and back of the cell allowed the visual observation of phase transitions that occurred inside the equilibrium cell. The cell content was vigorously agitated by an impeller-type stirrer. A thermocouple with an accuracy of ±0.1 K for full ranges was inserted into the cell to measure the temperature of the inner content. This thermocouple was calibrated using an ASTM 63C mercury thermometer (Ever Ready Thermometer, USA) with a resolution of ±0.1 K. A pressure transducer (S-10, Wika, Germany) with an uncertainty of 0.01 MPa was used to measure cell pressure. The pressure transducer was also calibrated using a Heise Bourdon tube pressure gauge (CMM-137219, 0 to 10 MPa range) having a maximum error of ±0.01 MPa in the full range.

The experiment for hydrate phase equilibrium measurements began with charging the equilibrium cell with about 80 cm^3 of 2-PrOH solution. Before each experimental run, the equilibrium cell was flushed at least three times with the hydrate-forming gas to remove any residual air. After the equilibrium cell was pressurized to the desired pressure with CH_4 or CO_2, the whole main system was slowly cooled to a temperature lower than the expected equilibrium temperature. Because of thermal contraction, the cell pressure was slightly decreased by decreasing the temperature at a cooling rate of 1.0 K steps in 60 min. Then, an abrupt pressure depression was observed at the stage of hydrate crystal growth after nucleation. When the pressure depression due to hydrate formation reached a steady-state condition, the temperature was increased in 0.1 K steps in 90 min, and accordingly, the cell pressure was increased with hydrate dissociation. After all the hydrates were dissociated with increasing temperature, the cell pressure was again slightly increased due to thermal expansion. Pressure and temperature points at 90 min of each step were collected, and then, the final dissociation and thermal expansion lines were obtained. The H−L_W−V equilibrium points at each pressure condition were determined from the intersection between the hydrate dissociation and thermal expansion lines.

The hydrate samples for PXRD and NMR analyses were prepared with the same apparatus as that used for hydrate phase equilibrium measurements. When the hydrate formation was completed, the formed hydrates were finely powdered in a liquid nitrogen vessel for measurements. The structure of the double CH_4 + 2-PrOH and CO_2 + 2-PrOH hydrates was determined by a Rigaku Geigerflex diffractometer (D/Max-RB) by using graphite-monochromatized Cu Kα1 radiation (λ = 1.5406 Å). The XRD data were collected by step mode with a fixed time of 3 s and a step size of 0.02° for 2θ = 10−60° at 123.15 K. The obtained patterns were analyzed by the Checkcell program.

A Bruker 400 MHz solid-state NMR spectrometer that belongs to the Korea Basic Science Institute (KBSI) was used in order to reveal cage occupancies and guest distributions in the double CH_4 + 2-PrOH hydrates. The NMR spectra were recorded at 243 K and atmospheric pressure by placing the hydrate samples within a 4 mm o.d. Zr rotor that was loaded into the variable-temperature (VT) probe. All ^{13}C NMR spectra were recorded at a Larmor frequency of 100.6 MHz with magic angle spinning (MAS) between 2 and 4 kHz. A pulse length of 2 μs and pulse repetition delay of 10 s under proton decoupling were employed when a radio frequency field strength of 50 kHz corresponding to 5 μs 90° pulses were used. The downfield carbon resonance peak of adamantane, which was assigned a chemical shift of 38.3 ppm at 300 K, was used as an external chemical shift reference. A more detailed description of the experimental methods has been provided in previous papers.[17−19]

RESULTS AND DISCUSSION

In the pressurization of CH_4, 2-PrOH works as a guest of sII double hydrates and can promote hydrate stability conditions due to the inclusion of 2-PrOH in the large $5^{12}6^4$ cages.[11,12] Therefore, in this study, the phase behavior, structural transition, and guest distributions that resulted from the enclathration of 2-PrOH in the hydrate lattices were examined in the presence of help gases such as CH_4 and CO_2.

PXRD measurements were conducted in order to verify the crystal structure and the calculated cell parameters of the double hydrates of 2-PrOH with CH_4 and CO_2. Figure 1 shows the PXRD patterns for the double CH_4 + 2-PrOH (5.6 mol %) and double CO_2 + 2-PrOH (5.6 mol %) hydrates. The double CH_4 + 2-PrOH hydrate was identified as a sII crystal structure and can be indexed using a regular cubic unit cell ($Fd3m$) with a unit cell parameter of 17.30 Å. This value is in good agreement with the previously reported value.[12] The double CO_2 + 2-PrOH hydrate was also found to be a cubic ($Fd3m$) sII structure with a unit cell parameter of 17.31 Å. The characterization of the double CO_2 + 2-PrOH hydrate via PXRD was first accomplished in this study, and the value of the cell parameter was almost identical to that of the double CH_4 +

dx.doi.org/10.1021/jp310487w | J. Phys. Chem. B 2013, 117, 2449−2455

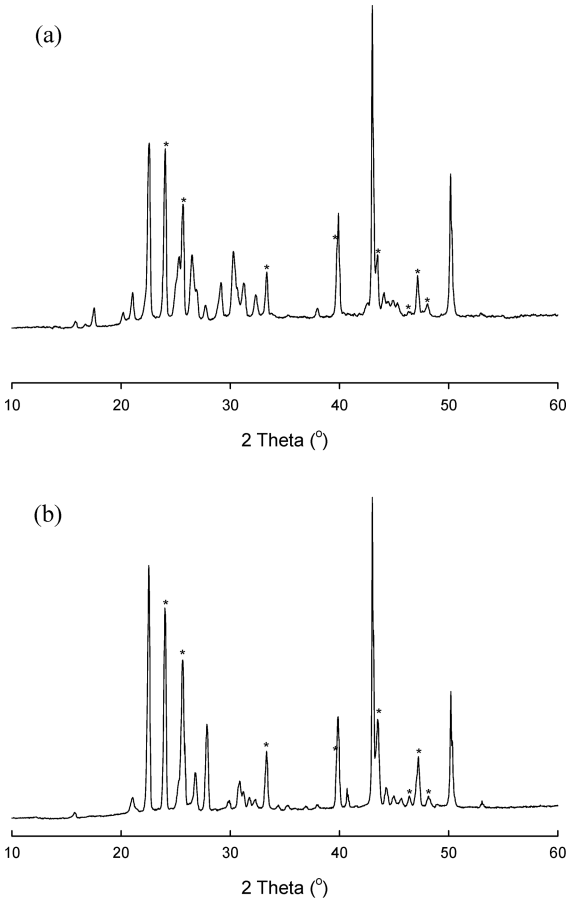

Figure 1. (a) PXRD pattern of the double CH_4 + 2-PrOH (5.6 mol %) hydrate and (b) PXRD pattern of the double CO_2 + 2-PrOH (5.6 mol %) hydrate. Asterisks indicate the hexagonal ice (Ih) phase.

Table 1. Hydrate Phase Equilibrium Data for the CH_4 + 2-PrOH + Water Systems

1.0 mol %		5.6 mol %		10.0 mol %		15.0 mol %	
T (K)	P (MPa)	T (K)	P (MPa)	T (K)	P (MPa)	T (K)	P (MPa)
273.5	2.58	275.5	2.56	274.6	2.69	274.4	2.98
277.9	4.16	279.8	4.16	277.9	3.95	277.8	4.33
281.2	5.93	283.1	5.92	281.1	5.72	280.3	5.81
283.7	7.75	284.9	7.69	283.2	7.13	282.4	7.32
285.7	10.09	286.4	9.19	285.1	9.27	284.0	8.85

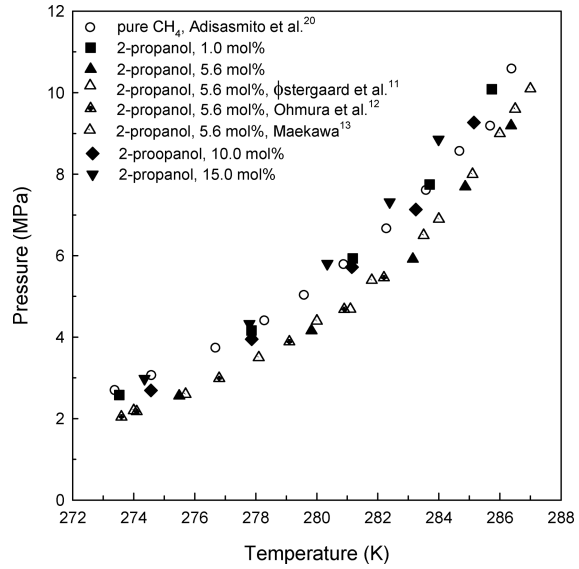

Figure 2. Hydrate phase equilibria of the CH_4 + 2-PrOH + water mixtures.

2-PrOH hydrate. The PXRD results indicate that, in the presence of CH_4 and CO_2, sII hydrate formation was induced via the enclathration of 2-PrOH molecules in the large $5^{12}6^4$ cages.

Thermodynamic studies, particularly on hydrate stability regions, are very important in estimating and predicting the pressure and temperature conditions required for the hydrate formation and dissociation. The shift of the H−L_W−V equilibrium lines due to the addition of chemical compounds to the systems is generally caused by either the thermodynamic promotion resulting from the added compounds occupying the hydrate cages or the thermodynamic inhibition resulting from the added compounds disrupting the hydrogen bonding network of water. In this study, the three-phase (H−L_W−V) equilibria for the CH_4 + 2-PrOH + water and CO_2 + 2-PrOH + water mixtures were experimentally measured at four different 2-PrOH concentrations of 1.0, 5.6, 10.0, and 15.0 mol % in order to determine the stability conditions of the double 2-PrOH hydrates.

The overall experimental results are summarized in Table 1 and presented in Figure 2 with the relevant reference data.[11−13,20] As seen in Figure 2, the H−L_W−V equilibrium conditions of the double CH_4 + 2-PrOH hydrates were shifted to the stabilized regions that are represented by higher temperatures and lower pressure conditions when compared with the pure CH_4 hydrate system. The stabilizing effect of 2-PrOH was remarkable for the solution with 2-PrOH 5.6 mol %, while only small stabilizing effects were observed for the solutions with 2-PrOH 1.0 mol % and 2-PrOH 10.0 mol %. As observed in other hydrate systems with water-soluble thermodynamic promoters, the maximum stabilizing effect occurs at the stoichiometric concentration of each hydrate structure formed by enclathrating thermodynamic promoters.[18,19,21,22] As revealed in the PXRD measurements, the CH_4 + 2-PrOH mixtures form a sII hydrate, and thus, the 2-PrOH 5.6 mol % corresponds to the stoichiometric concentration of the sII hydrate when the 2-PrOH molecules are assumed to occupy only the large $5^{12}6^4$ cages of the sII hydrate. The small promotion effect at 2-PrOH 1.0 mol % can be attributed to the lower cage occupancy of 2-PrOH in the large $5^{12}6^4$ cages of the sII hydrate. For the solutions with 2-PrOH 10.0 mol % and 15.0 mol %, only a stoichiometric amount of 2-PrOH engages in the double hydrate formation; thus, the remaining 2-PrOH molecules act as inhibitors, resulting in less stabilized conditions than the solution with the 2-PrOH 5.6 mol %. The stabilizing effect of 2-PrOH observed in the H−L_W−V equilibrium measurements indirectly indicates that the 2-PrOH molecules were captured in the hydrate cages, and this enclathration of 2-PrOH leads to the structural transformation of the pure sI CH_4 gas hydrate into the double sII CH_4 + 2-PrOH hydrate.

The three-phase H−L_W−V equilibria for the CO_2 + 2-PrOH + water systems exhibited a significantly different trend from those for the CH_4 + 2-PrOH + water systems. The double CO_2 + 2-PrOH hydrate systems were more inhibited when the 2-PrOH concentration increased from 1.0 to 15.0 mol %. The

dx.doi.org/10.1021/jp310487w | J. Phys. Chem. B 2013, 117, 2449−2455

overall experimental results for the double CO_2 + 2-PrOH hydrate are summarized in Table 2 and shown in Figure 3. The

Table 2. Hydrate Phase Equilibrium Data for the CO_2 + 2-PrOH + Water Systems

1.0 mol %		5.6 mol %		10.0 mol %		15.0 mol %	
T (K)	P (MPa)	T (K)	P (MPa)	T (K)	P (MPa)	T (K)	P (MPa)
274.1	1.50	274.3	2.50	273.1	2.94	272.5	2.98
276.2	1.87	275.7	2.90	273.4	3.05	273.0	3.15
277.8	2.32	276.2	3.13	273.8	3.19	273.4	3.28
279.5	2.94	276.8	3.34	274.7	3.46		
281.2	3.51	277.4	3.58				
282.2	4.11	278.3	3.89				

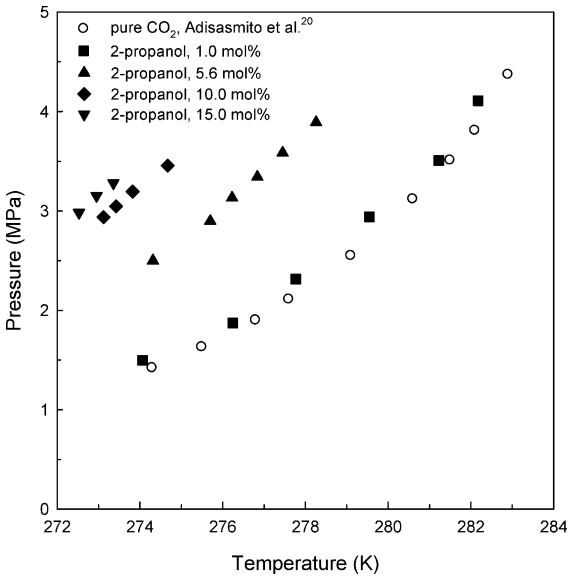

Figure 3. Hydrate phase equilibria of the CO_2 + 2-PrOH + water mixtures.

apparent inhibition effects were observed with the addition of 2-PrOH to the CO_2 + water systems, even though the PXRD measurements demonstrated that the CO_2 + 2-PrOH + water systems form sII hydrates due to the inclusion of 2-PrOH in the hydrate lattices. Generally, the inclusion of large-sized guest molecules in the hydrate cages causes the hydrate system to be more stabilized, as is commonly observed in thermodynamic promoter-added systems.[18,19,21,22] However, some recent investigations also have reported that H−L_W−V equilibrium lines can be shifted to the inhibition regions despite the inclusion of large guest molecules and the subsequent structural transition.[7,23] The apparent inhibition due to the addition of 2-PrOH to the CO_2 hydrate systems is related to the cage occupancy of guest molecules in the hydrate cages and the hydrogen bonding between guest and host molecules. As indicated by previous researchers,[5,6] the alcohol occupancy in the double CO_2 + alcohol hydrates is relatively lower than that in the double CH_4 + alcohol hydrates. In addition, because of the molecular size, CO_2 is a relatively poorer guest for the small 5^{12} cages of sII hydrates when compared with CH_4. Accordingly, the lower occupancies of both 2-PrOH molecules in the large $5^{12}6^4$ cages and CO_2 molecules in the small 5^{12} cages of the double CO_2 + 2-PrOH hydrates result in less thermodynamic stability. Furthermore, Alavi et al.[6] noted in the results of their molecular dynamics simulations that the probability of guest−water hydrogen bonding in the double CO_2 + alcohol hydrates is significantly greater than that in the double CH_4 + alcohol hydrates. Strong guest−water hydrogen bonding can disrupt the hydrogen bonding network of the host, which can result in hydrate instability. Therefore, when compared with the CH_4 + 2-PrOH hydrates, lower guest occupancy in both the small 5^{12} and large $5^{12}6^4$ cages and stronger guest−host hydrogen bonding could explain the experimentally observed H−L_W−V equilibrium line shift to the inhibition regions with increasing 2-PrOH concentrations in the double CO_2 + 2-PrOH hydrates.

^{13}C MAS NMR measurements were undertaken in order to confirm the hydrate structure and to examine the guest distributions in the double CH_4 + 2-PrOH hydrates. The cage-dependent ^{13}C NMR chemical shifts for the enclathrated CH_4 molecules can be used effectively to determine the structure types of the formed gas hydrates.[24] Figure 4a shows a stacked plot of the ^{13}C MAS NMR spectra of the pure CH_4 hydrate, double CH_4 + 2-PrOH (1.0 mol %) hydrate, and double CH_4 + 2-PrOH (5.6 mol %) hydrate, and Figure 4b presents the resonance peaks from the CH_4 molecules captured in the hydrate structure made from the 2-PrOH 1.0 mol % solution in the upfield region of 0 to −10 ppm. The spectrum of the CH_4 hydrate that is known to form the sI had two resonance peaks at −4.3 and −6.6 ppm. The peak at −4.3 ppm can be assigned to the CH_4 molecules in the small 5^{12} cages, and the peak at −6.6 ppm can be assigned to the CH_4 molecules in the large $5^{12}6^2$ cages, considering the ideal stoichiometric ratio of the small 5^{12} to the large $5^{12}6^2$ cages in the unit cell of the sI. The double CH_4 + 2-PrOH (5.6 mol %) hydrate exhibited three significant resonance peaks at −4.5, 26.4, and 63.6 ppm. The signal at −4.5 ppm denotes the CH_4 molecules captured in the large $5^{12}6^4$ cages of the sII. The 2-PrOH molecules captured only in the large $5^{12}6^4$ cages due to the size limitations were identified by two distinct signals: one from $-CH_3$ (at 26.4 ppm) and the other from −CH− (at 63.6 ppm). However, additional signals, which can be assigned to the 2-PrOH hydrate that was formed from unreacted 2-PrOH molecules, were observed around each main peak.

In the 2-PrOH 1.0 mol % solution, a considerable amount of the pure CH_4 hydrate (sI) was observed as well as the double CH_4 + 2-PrOH hydrate (sII), as shown in Figure 4b. The pressure and temperature conditions for preparing the double gas hydrate sample with 2-PrOH 1.0 mol % was also sufficient for the pure CH_4 gas hydrate to form because the two H−L_W−V equilibrium lines are located very close to each other, as seen in Figure 2. For water-soluble or insoluble sII hydrate-forming guests, the coexistence of sI and sII hydrates was commonly observed at concentrations lower than the stoichiometry, and this resulted from the additional reaction of CH_4 with the unreacted water.[21−23] Again, the resonance peaks at −4.3 and −6.6 ppm demonstrate the CH_4 molecules captured in the small 5^{12} and large $5^{12}6^2$ cages of the sI hydrate, respectively, while the resonance peaks at −4.5 and −8.2 ppm represent the CH_4 molecules in the small 5^{12} and large $5^{12}6^4$ cages of the sII hydrate, respectively. Only a very slight difference between the chemical shifts of the two CH_4 signals from the small 5^{12} cages of sI and sII was observed because both small cages of sI and sII consist of the pentagonal dodecahedra (5^{12}) with nearly the same dimensions.[1] However, the chemical shifts of the CH_4 molecules in the large $5^{12}6^2$ (−6.6 ppm) and $5^{12}6^4$ (−8.2 ppm) cages of sI and sII, respectively, demonstrated a distinctive

dx.doi.org/10.1021/jp310487w | J. Phys. Chem. B 2013, 117, 2449−2455

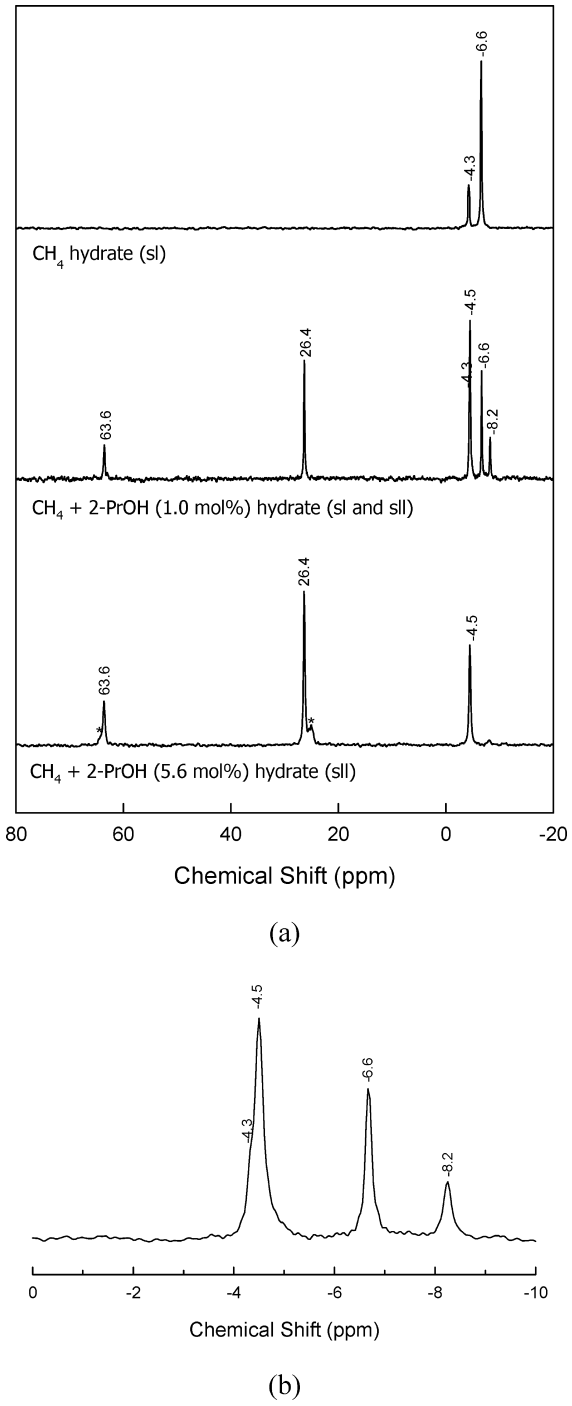

Figure 4. (a) ^{13}C NMR spectra of the pure CH_4, double CH_4 + 2-PrOH (1.0 mol %), and double CH_4 + 2-PrOH (5.6 mol %) hydrates and (b) ^{13}C NMR spectrum of the double CH_4 + 2-PrOH (1.0 mol %) hydrate in the upfield region. Asterisks indicate the resonance peaks from the 2-PrOH hydrate.

discrepancy for the enclathrated CH_4 molecules because the size and shape of large cages of the each hydrate structure are quite different.[1] Accordingly, the CH_4 chemical shift pattern of the large cages of each hydrate structure can be used as a clear indicator for determining the structure types of the gas hydrates formed.

From the ^{13}C NMR spectra of the double CH_4 + 2-PrOH hydrates, it should be noted that the guest distribution is clearly affected by the 2-PrOH concentration. Lee and Kang[7] indicated that, in the double CH_4 + ethanol hydrates, the large $5^{12}6^4$ cages of the sII hydrates are always shared by both ethanol and CH_4 molecules, even at the stoichiometric ethanol concentration as well as at lower ethanol concentrations. However, in the double CH_4 + 2-PrOH hydrates of this study, the large $5^{12}6^4$ cages were occupied solely by the 2-PrOH molecules at the stoichiometric 2-PrOH concentration, while the large $5^{12}6^4$ cages were shared by both CH_4 and 2-PrOH molecules at the lower 2-PrOH concentration (1.0 mol %). The cage occupancies of each component in the double CH_4 + 2-PrOH hydrates were calculated using the relative integrated peak areas of the ^{13}C MAS NMR signals at each chemical shift combined with the following statistical thermodynamic expression that represents the chemical potential of water molecules:[25]

$$\mu_W(h) - \mu_W(h^0) = \frac{RT}{17}[\ln(1 - \theta_{l,2\text{-PrOH}} - \theta_{l,CH_4}) + 2\ln(1 - \theta_{s,CH_4})]$$

where $\mu_W(h^0)$ is the chemical potential of the water molecules of a hypothetical empty lattice, and θ_s and θ_l are the fractional occupancies of the small and large cages, respectively. When the gas hydrate is in equilibrium with the ice, the left side of the above equation becomes $\mu_W(\text{ice}) - \mu_W(h^0) = -\Delta\mu_W^0$, where $\Delta\mu_W^0$ is the chemical potential of the empty lattice relative to the ice. The value of $\Delta\mu_W^0$ used in this study is 883.8 J/mol for sII.[1] The integrated area ratios of the guest CH_4 to 2-PrOH molecules were substituted in the above equations in order to calculate the cage occupancies of each molecule; the results are listed in Table 3 and Figure 5. As seen from Table 3 and Figure 5, the CH_4 occupancy in the small 5^{12} cages was almost constant (0.79 to 0.75) with an increasing 2-PrOH concentration from 1.0 to 5.6 mol %, while the 2-PrOH occupancy in the large $5^{12}6^4$ cages significantly increased (0.55 to 0.98) with an increasing 2-PrOH concentration from 1.0 to 5.6 mol %. The decreased 2-PrOH occupancy in the large $5^{12}6^4$ cages at the lower 2-PrOH concentration was attributed to the considerable CH_4 occupancy in the large $5^{12}6^4$ cages. The double CH_4 + 2-PrOH hydrates exhibited much higher alcohol occupancy in the large $5^{12}6^4$ cages of sII for all concentration ranges when compared with the double CH_4 + ethanol hydrates.[7] The higher 2-PrOH occupancy in the large $5^{12}6^4$ cages can explain the more stabilized hydrate equilibrium conditions of the double CH_4 + 2-PrOH hydrates compared with those of the double CH_4 + ethanol hydrates. The cage occupancies of the guest molecules obtained from the NMR analysis yielded a chemical formula of $1.99CH_4 \cdot 0.55$ 2-PrOH$\cdot 17\ H_2O$ at 2-PrOH 1.0 mol % and $1.50CH_4 \cdot 0.98$ 2-PrOH$\cdot 17\ H_2O$ at 2-PrOH 5.6 mol %. The exact cage filling characteristics and chemical formula of the double CH_4 + 2-PrOH hydrates are presented first in this study. The experimental results obtained in this study indicate that the guest gas distribution and the composition of the double CH_4 +

Table 3. Cage Occupancies of the Double CH_4 + 2-PrOH Hydrates

	CH_4		2-PrOH
system	θ_{s,CH_4}	θ_{l,CH_4}	$\theta_{l,2\text{-PrOH}}$
CH_4 + 2-PrOH (1.0 mol %)	0.79	0.41	0.55
CH_4 + 2-PrOH (5.6 mol %)	0.75	0	0.98

dx.doi.org/10.1021/jp310487w | J. Phys. Chem. B 2013, 117, 2449−2455

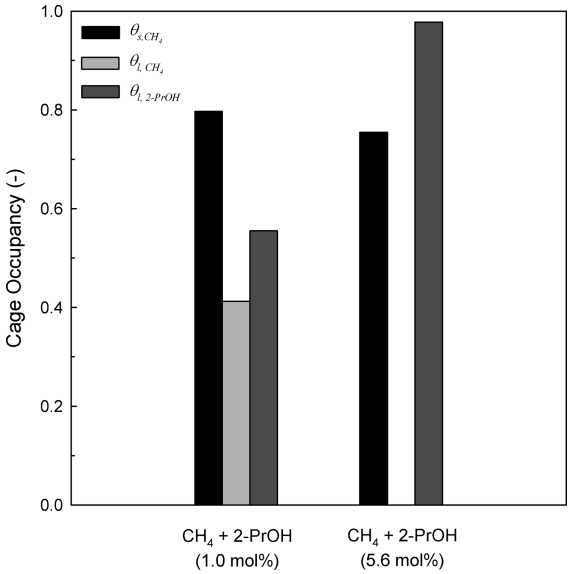

Figure 5. Cage occupancies of the CH_4 and 2-PrOH molecules in the double CH_4 + 2-PrOH hydrates at two different 2-PrOH concentrations of 1.0 and 5.6 mol %.

2-PrOH hydrates can be altered with adjustments in the 2-PrOH concentration.

CONCLUSIONS

Phase behavior, structural transition, and guest distributions of the 2-PrOH double hydrates with CH_4 and CO_2 were examined through macroscopic equilibrium measurements and microscopic analyses using PXRD and solid-state NMR. From the PXRD patterns, it was found that both the double CH_4 + 2-PrOH hydrate and double CO_2 + 2-PrOH hydrate have cubic sII crystal structures. When compared with the pure hydrate system, the CH_4 + 2-PrOH hydrate systems demonstrated stabilized H–L_W–V equilibrium conditions, while the CO_2 + 2-PrOH hydrate systems exhibited inhibited H–L_W–V equilibrium conditions despite the enclathration of the 2-PrOH molecules in the large $5^{12}6^4$ cages of the sII hydrates. It was confirmed from the ^{13}C NMR spectra that, at a 2-PrOH concentration lower than stoichiometry, the small 5^{12} cages were occupied by CH_4 molecules only, whereas the large $5^{12}6^4$ cages were shared by the CH_4 and 2-PrOH molecules. However, at the stoichiometric concentration, the large $5^{12}6^4$ cages were occupied by the 2-PrOH molecules only, and the corresponding chemical formula for the stoichiometric concentration is $1.50CH_4 \cdot 0.98$ 2-PrOH$\cdot 17H_2O$. The overall experimental results obtained in this study are very useful for understanding the guest distributions, guest–host interactions, and structural details of the guest gas + 2-PrOH hydrates and thus could be valuable information for the potential application of 2-PrOH in gas storage and transportation.

ASSOCIATED CONTENT

Supporting Information

^{13}C NMR spectra of the liquid 2-PrOH and 2-PrOH hydrate. This material is available free of charge via the Internet at http://pubs.acs.org.

AUTHOR INFORMATION

Corresponding Author

*Tel: +82-52-217-2821. Fax: +82-52-217-2819. E-mail: ywseo@unist.ac.kr.

Notes

The authors declare no competing financial interest.

ACKNOWLEDGMENTS

This research was supported by Basic Science Research Program through the National Research Foundation of Korea (NRF) funded by the Ministry of Education, Science, and Technology (2012-002494) and also supported by the Future Creativity and Innovation project (2012) of the UNIST (1.120022.01).

REFERENCES

(1) Sloan, E. D.; Koh, C. A. *Clathrate Hydrates of Natural Gases*, 3rd ed.; CRC Press: Boca Raton, FL, 2008.

(2) Koh, C. A.; Sloan, E. D.; Sum, A. *Natural Gas Hydrates in Flow Assurance*; Gulf Professional Publishing: Burlington, MA, 2011.

(3) Yasuda, K.; Takeya, S.; Sakashita, M.; Yamawaki, H.; Ohmura., R. Binary Ethanol–Methane Clathrate Hydrate Formation in the System CH_4–C_2H_5OH–H_2O: Confirmation of Structure II Hydrate Formation. *J. Phys. Chem. C* **2009**, *113*, 12598–12601.

(4) Anderson, R.; Chapoy, A.; Haghighi, H.; Tohidi, B. Binary Ethanol–Methane Clathrate Hydrate Formation in the System CH_4-C_2H_5OH-H_2O: Phase Equilibria and Compositional Analyses. *J. Phys. Chem. C* **2009**, *113*, 12602–12607.

(5) Makiya, T.; Murakami, T.; Takeya, S.; Sum, A. K.; Alavi, S.; Ohmura, R. Synthesis and Characterization of Clathrate Hydrates Containing Carbon Dioxide and Ethanol. *Phys. Chem. Chem. Phys.* **2010**, *12*, 9927–9932.

(6) Alavi, S.; Ohmura, R.; Ripmeester, J. A. A Molecular Dynamic Study of Ethanol–Water Hydrogen Bonding in Binary Structure I Clathrate Hydrate with CO_2. *J. Chem. Phys.* **2011**, *134*, 054702.

(7) Lee, J.-W.; Kang, S.-P. Spectroscopic Identification on Cage Occupancies of Binary Gas Hydrates in the Presence of Ethanol. *J. Phys. Chem. B* **2012**, *116*, 332–335.

(8) Park, Y.; Cha, M.; Shin, W.; Lee, H.; Ripmeester, J. A. Spectroscopic Observation of Critical Guest Concentration Appearing in *tert*-Butyl Alcohol Clathrate Hydrate. *J. Phys. Chem. B* **2008**, *112*, 8443–8446.

(9) Chapoy, A.; Anderson, R.; Haghighi, H.; Edward, T.; Tohidi, B. Can *n*-Propanol Form Hydrate? *Ind. Eng. Chem. Res.* **2008**, *47*, 1689–1694.

(10) Yasuda, K.; Takeya, S.; Sakashita, M.; Yamawaki, H.; Ohmura, R. Characterization of the Clathrate Hydrate Formed with Methane and Propan-1-ol. *Ind. Eng. Chem. Res.* **2009**, *48*, 9335–9337.

(11) Østergaard, K.; Tohidi, B.; Anderson, R.; Todd, A. C.; Danesh, A. Can 2-Propanol Form Clathrate Hydrates? *Ind. Eng. Chem. Res.* **2002**, *41*, 2064–2068.

(12) Ohmura, R.; Takeya, S.; Uchida, T.; Ebinuma, T. Clathrate Hydrates Formed with Methane and 2-Propanol: Confirmation of Structure II Hydrate Formation. *Ind. Eng. Chem. Res.* **2004**, *43*, 4964–4966.

(13) Maekawa, T. Equilibrium Conditions for Clathrate Hydrates Formed from Methane and Aqueous Propanol Solutions. *Fluid Phase Equilib.* **2008**, *267*, 1–5.

(14) Alavi, S.; Takeya, S.; Ohmura, R.; Woo, T. K.; Ripmeester, J. A. Hydrogen-Bonding Alcohol–Water Interactions in Binary Ethanol, 1-Propanol, and 2-Propanol + Methane Structure II Clathrate Hydrates. *J. Chem. Phys.* **2010**, *133*, 074505.

(15) Zhurko, F. V.; Manakov, A. Y.; Kosyakov, V. Formation of Gas Hydrates in the Systems Methane–Water–ROH (ROH = Ethanol, *n*-Propanol, *i*-Propanol, *i*-Butanol). *Chem. Eng. Sci.* **2010**, *65*, 900–905.

(16) Aladko, L. S.; Manakov, A. Y.; Ogienko, A. G.; Ancharov, A. I. New Data on Phase Diagram and Clathrate Formation in the System

Water−Isopropyl Alcohol. *J. Inclusion Phenom. Macrocyclic Chem.* **2009**, *63*, 151−157.
(17) Lee, S.; Seo, Y. Experimental Measurement and Thermodynamic Modeling of the Mixed CH_4 + C_3H_8 Clathrate Hydrate Equilibria in Silica Gel Pores: Effects of Pore Size and Salinity. *Langmuir* **2010**, *26*, 9742−9748.
(18) Lee, S.; Park, S.; Lee, Y.; Lee, J.; Lee, H.; Seo, Y. Guest Gas Enclathration in Semiclathrates of Tetra-*n*-butylammonium Bromide: Stability Condition and Spectroscopic Analysis. *Langmuir* **2011**, *27*, 10597−10603.
(19) Lee, S.; Lee, Y.; Park, S.; Kim, Y.; Lee, J. D.; Seo, Y. Thermodynamic and Spectroscopic Identification of Guest Gas Enclathration in the Double Tetra-*n*-butylammonium Fluoride Semiclathrates. *J. Phys. Chem. B* **2012**, *116*, 9075−9081.
(20) Adisasmito, S.; Frank, R. J.; Sloan, E. D. Hydrates of Carbon Dioxide and Methane Mixtures. *J. Chem. Eng. Data* **1991**, *36*, 68−71.
(21) Kim, D.-Y.; Park, J.; Lee, J.-W.; Ripmeester, J. A.; Lee, H. Critical Guest Concentration and Complete Tuning Pattern Appearing in the Binary Clathrate Hydrates. *J. Am. Chem. Soc.* **2006**, *128*, 15360−15361.
(22) Seo, Y.; Lee, J.-W.; Kumar, R.; Moudrakovski, I.; Lee, H.; Ripmeester, J. A. Tuning the Composition of Guest Molecules in Clathrate Hydrates: NMR Identification and Its Significance to Gas Storage. *Chem. Asian J.* **2009**, *4*, 1266−1274.
(23) Shin, W.; Park, S.; Koh, D.-Y.; Seol, J.; Lee, J.-W.; Seo, Y.; Lee, H. Structure Transition from Semi- to True Clathrate Hydrates Induced by CH_4 Enclathration. *J. Phys. Chem. C* **2012**, *116*, 16352−16357.
(24) Ripmeester, J. A.; Ratcliffe, C. I. On the Contributions of NMR Spectroscopy to Clathrate Science. *J. Struct. Chem.* **1999**, *40*, 654−662.
(25) van der Waals, J. H.; Platteeuw, J. C. Clathrate Solutions. *Adv. Chem. Phys.* **1959**, *2*, 1−58.